Case Studies in Nondestructive Testing and Evaluation 6 (2016) 104–110

Contents lists available at ScienceDirect

Case Studies in Nondestructive Testing and Evaluation

www.elsevier.com/locate/csndt

Influence of surface roughness on X-ray computed tomography dimensional measurements of additive manufactured parts

Valentina Aloisi *, Simone Carmignato

University of Padova, Department of Management and Engineering, Stradella San Nicola, 3, 36100 Vicenza, Italy

ARTICLE INFO

Article history:
Available online 13 May 2016

ABSTRACT

In many industrial applications, components characterized by high surface roughness are measured by X-ray computed tomography (CT). This is the case, for example, of additive manufactured parts. Surface roughness has a strong influence on CT dimensional measurements, causing relevant measurement deviations with respect to tactile reference measurements by coordinate measuring machines (CMMs), especially for parts characterized by high surface roughness. It comes that roughness effects on CT dimensional measurements must be quantified.

In this work, the influence of surface roughness on CT dimensional measurements, and the relation between tactile CMM and CT measurements are studied. Effects of larger as well as smaller surface roughness are taken into account, by means of three different additive manufactured samples characterized by different roughness. Experimental results prove the presence of a systematic error between tactile and CT measurements; the relation between this error and the *Rz* roughness parameter of the surface is analyzed.

1. Introduction

X-ray computed tomography (CT) has been increasingly used in industry for dimensional quality control purposes [1]. It offers unique advantages compared to traditional measuring techniques, enabling dimensional analysis in a non-contact way on a wide variety of components. Often workpieces with high surface roughness are scanned; this is the case for example of additive manufactured parts. Surface roughness has a strong influence on CT dimensional measurements causing a considerable increase of uncertainty especially for parts characterized by high surface roughness [2,3]. The problem of how to treat roughness uncertainty contribution, therefore, is crucial for CT applications. At the state of the art, there are no internationally accepted standards for determination of measurement uncertainty for CT measurements. The experimental approach outlined in ISO 15530-3 [4] for coordinate measuring machines (CMMs) can be adapted also to CT, as proposed in several previous works [2,5–9]. According to the method specified in ISO 15530-3, the uncertainty component associated with the influence of the workpiece (e.g. surface roughness), namely u_w, contributes to the expanded uncertainty. It comes that roughness effects on CT dimensional measurements must be quantified and taken into account for measurement uncertainty determination.

* Corresponding author.
E-mail addresses: valentina.aloisi@dii.unipd.it (V. Aloisi), simone.carmignato@unipd.it (S. Carmignato).

http://dx.doi.org/10.1016/j.csndt.2016.05.005

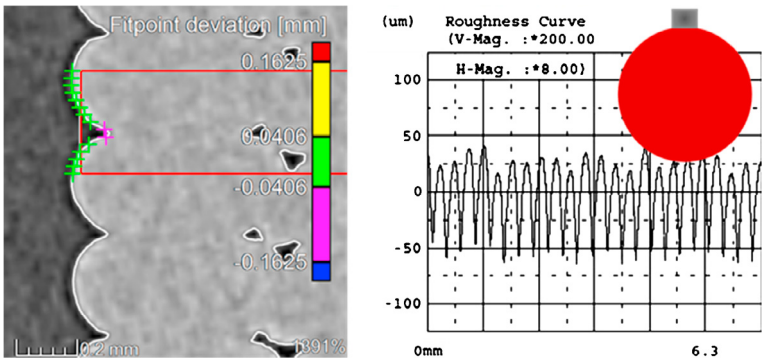

Fig. 1. Comparison between points acquired by CT and CMM on the surface of a cylindrical workpiece produced by FDM, with a *Rz* of 100 µm. (a) Points acquired by CT are distributed on the peaks and on the valleys of the profile. (b) Points acquired by CMM are only on the parts of the surface that can be touched by the probe; i.e. on the peaks of the profile. The image on the right shows the roughness curve measured on the cylindrical workpiece with a contact roughness tester. A schematic representation of a tactile CMM probe with a diameter of 3 mm is there superimposed (shown in red color) to illustrate the mechanical filtering effect it produces. The profile acquired by means of tactile measurement, therefore, is shifted toward roughness peaks.

In a previous work by Schmitt and Niggemann [2], uncertainty of CT dimensional measurements was assessed for a workpiece with roughness value *Rz* in the range of 6 µm. There, the authors proposed to estimate surface roughness effects on the basis of averaged *Rz* (maximum peak to valley height of the profile in the sampling length) measurements and assuming that the surface lies half within the part material. Bartscher et al. [10] estimated effects of less than a quarter of *Rz* for a workpiece with *Rz* up to 134 µm. Boeckmans et al. [11] showed that surface roughness offsets equal to *Rp* (maximum peak height of the profile in the sampling length) were found for turned aluminum cylinders.

In this work, the influence of surface roughness on CT dimensional measurements, and the relation between tactile CMM and CT measurements are investigated for different types of surfaces on additive manufactured parts with different roughness values. Repeated scans of calibrated workpieces produced by different additive manufacturing processes are performed with different voxel sizes. Roughness values *Rz* ranging from 30 µm to 125 µm are considered, to take into account the effects of lower as well as higher surface roughness. A systematic error caused by surface roughness is determined. Measurement uncertainty is then calculated according to the experimental approach derived from ISO 15530-3.

2. Deviations between CT and tactile CMM measurements due to surface roughness

While dealing with the application of computed tomography for dimensional metrology, tactile CMM measurements are often used as reference values and compared to CT measurements [12]. In fact, due to a well-established knowledge and the presence of internationally accepted standards for CMMs performance verification [13] and determination of measurement uncertainty [4], tactile CMMs can provide traceable measurements and several methods exist for accuracy enhancement [14]. However, the different measuring principles on which tactile CMMs and CT systems rely cannot be neglected. Due to the different acquisition principle, surface roughness may produce significant deviations between tactile CMM and CT measurement results.

Tactile CMMs acquire points by means of the mechanical contact between the probe stylus tip and the surface of the workpiece under investigation. Probing points can be acquired by different strategies (e.g. point by point or in scanning mode), with a point density which depends on user settings. On the other hand, the measuring principle of CT is based on the attenuation of X-rays. A 3-D voxel model is reconstructed, in which a grey value is attributed to each voxel depending on the X-ray absorption coefficient of the material and the path followed by the X-rays.

For example, Fig. 1 illustrates the differences between points acquired by CT and by tactile CMM on a cylindrical workpiece produced by Fused Deposition Modelling (FDM), and characterized by *Rz* values up to 125 µm.

In the example shown in Fig. 1, diameter measurements of the cylindrical workpiece were performed on the CT volume with a voxel size of 19 µm (Fig. 1-a); they show how the fit points for the diameter calculation are distributed on the whole profile, including peaks and valleys. Fig. 1-b represents the roughness profile of the same workpiece, measured with a tactile roughness tester with a 5 µm stylus tip. A CMM spherical probe with a 3 mm diameter is there superimposed, to represent the same conditions used during CMM measurement. Due to the finite dimensions of the probe, the acquired probing points cannot reach the valleys of the profile. The mechanical filtering effect increases with the size of the probe.

This means that tactile CMMs perform a mechanical low-pass filtering on the surface of the component. Acquired probing points lie on the peaks of the surface profile. For tactile measurements, therefore, the acquired profile is shifted towards roughness peaks. Computed tomography, instead, when using sufficiently small voxel sizes compared to the measured surface roughness, as well as small focal spot sizes, takes into account also lower wavelengths, allowing to virtually probe also points on the valleys of the profile [15]. Surface roughness, therefore, may produce systematic effects between tactile CMM measurements and CT measurements.

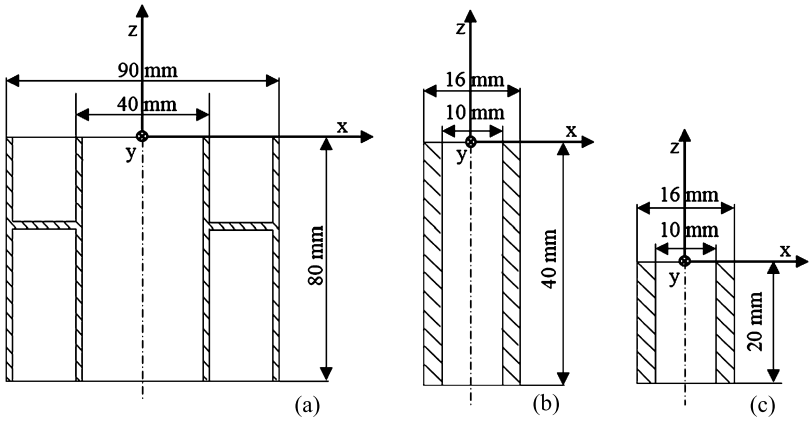

Fig. 2. Nominal dimensions of the workpieces used in the experimental investigation: (a) Sample 1, produced by SLS and made of steel; (b) Sample 2, produced by FDM and made of ABS; (c) Sample 3, produced by FDM, made of ABS, and treated with acetone. Note: for better visibility, sample 1 is represented with a 1:2 scale, whereas samples 2 and 3 are represented with a 1:1 scale.

3. Experimental set-up

To investigate the influence of surface roughness on CT dimensional measurements, three different workpieces, produced by Additive Manufacturing technologies (AM) are considered in this study. Fig. 2 shows the nominal dimensions of the workpieces used for the experimental investigation.

Sample 1 (Fig. 2-a) is an industrial component, produced by Selective Laser Sintering (SLS) and made of steel. It features internal and external cylinders with nominal diameters ranging from 40 mm to 90 mm. Sample 2 and sample 3, instead, (Figs. 2-b and 2-c) are both produced by Fused Deposition Modelling (FDM), an AM technique in which a polymeric thermoplastic wire, in this case an ABS (Acrylonitrile Butadiene Styrene) wire, is heated and extruded and then added layer by layer to create the desired geometry. For the experimental investigation, sample 2 was left on its original state, while sample 3 was treated with acetone (C_3H_6O) in order to obtain a lower surface roughness.

All the three components were calibrated using a tactile CMM Zeiss Prismo VAST (maximum permissible error of length measurement equal to $2 + L/300$ µm, with L in mm). For each sample, 10 repeated CMM measurements were performed, with the reference system shown in Fig. 2. Different circular probing paths on different z coordinates were acquired in scanning mode using a ruby sphere probe with diameter of 3 mm. Approximately 1500 points per circle were acquired. External and internal diameters of the measured circles were calculated by means of Gaussian least-squares fitting.

Seven repeated CT scans were acquired for sample 1, on an industrial 2-D CT system, with a fan-beam geometry and a linear detector, using a voxel size of 120 µm. Five repeated CT scans, with a voxel size of 19 µm, were performed for each of the FDM samples (sample 2 and sample 3) using a metrological CT system (Nikon Metrology MCT 225).

Roughness measurements were performed by means of a contact roughness tester, Zeiss TSK Surfcom 1400, with a 5 µm stylus tip. The surface roughness was measured on different areas of the samples in order to obtain values representative for the whole surface. A total of 20 measurements per sample were performed. Cut-off filters λ_c and evaluation lengths were applied according to ISO 4288 [16].

Table 1 summarizes the average roughness values obtained for internal and external surfaces of the three samples. In particular, the *Rz* parameter is taken into account here, which is defined as the peak to valley height of the profile along the sampling length.

Table 1
Roughness measurements of components.

	External surface	Internal surface
Sample 1	$Rz = 125$ µm	$Rz = 100$ µm
Sample 2	$Rz = 114$ µm	$Rz = 125$ µm
Sample 3	$Rz = 33$ µm	$Rz = 34$ µm

By analyzing the roughness profile of sample 3 (Fig. 3-a) it can be noticed how the effect of the acetone treatment did not influence the periodicity of the profile, but just the heights of the peaks. The treatment caused a displacement of material from the peaks to the valleys, reducing therefore the *Rz* values (compared to the original state), without affecting the periodicity and bearing characteristics of the surface.

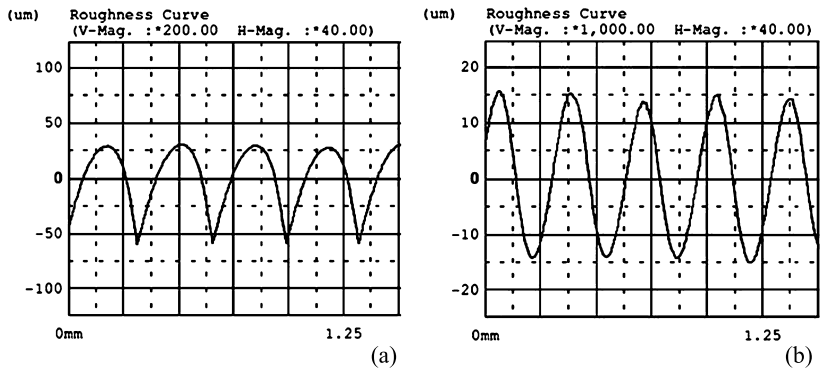

Fig. 3. Roughness profiles of sample 3: (a) before the treatment with acetone, (b) after the treatment with acetone. Note that the two diagrams have different scales in the vertical axis, for better visibility.

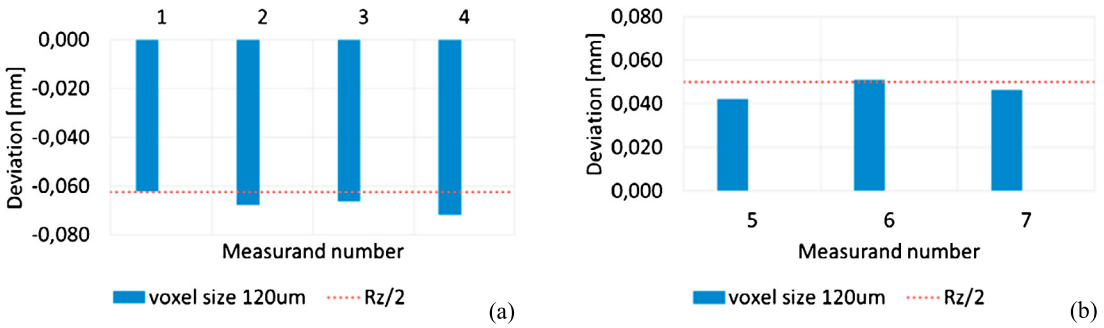

Fig. 4. (a) Deviations between CT and CMM measurements for external diameters of sample 1. Vertical columns represent the deviations for each measurand, while the horizontal axis represents the measurand number. The dashed line shows the value corresponding to $Rz/2$ of the external surface. (b) Deviations between CT and CMM measurements for internal diameters of sample 1. Vertical columns represent the deviations for each measurand, while the horizontal axis represents the measurand number. The dashed line shows the value corresponding to $Rz/2$ of the internal surface.

4. Results and discussion

All CT scans were imported and analyzed by means of the evaluation software VGStudio MAX 2.2 [17], using a local advanced surface determination method. For each sample, the same coordinate system used during CMM calibration was replicated. External and internal diameters were then measured at the same positions where the circular probing paths were acquired by the CMM. Each diameter was evaluated by fitting a cylinder with a height of 0.2 mm for each measurand of sample 1, and 0.33 mm for sample 2 and sample 3. Gaussian least-squares fitting was used as in the case of CMM measurements. Fitting a cylinder instead of a circle was necessary to simulate the same probing areas interested by CMM scanning.

Fig. 4 reports results obtained for sample 1. External diameters measured by CT are always smaller than the corresponding CMM measurements, with differences that are approximately equal to $Rz/2$. Internal diameters, instead, are always bigger than CMM reference values, with differences that in this case are also approximately $Rz/2$.

Figs. 5 and 6 show the biases between CT measurements and CMM reference values for external and internal diameters, respectively for sample 2 and 3. Also in these cases, as in Fig. 4, external and internal diameters show an opposite behavior, with differences of approximately $Rz/2$.

This systematic difference, approximately equal to $Rz/2$, is present for all diameter measurements in the three samples. The experimental results prove that also in the case of a smaller surface roughness, as in the case of sample 3, the difference between CT and CMM results is close to $Rz/2$. Attention is drawn to the fact that in this experimental investigation, all the three different surfaces that were analyzed (samples 1, 2 and 3) were characterized by similar bearing properties (i.e. similar Abbott–Firestone curve, which is also referred to as the bearing ratio curve or material ratio curve [18]). In this case, systematic differences of approximately $Rz/2$ were found between CT and CMM measurements. However, it is expected that the systematic shift between CT and CMM measurements is influenced by the Abbott–Firestone curve of the profile. In particular, systematic shifts smaller than $Rz/2$ are expected for surfaces with higher bearing curves (i.e. the material is more distributed on the peaks), whereas deviations higher that $Rz/2$ are expected for surfaces characterized by lower bearing properties (i.e. high percentage of material on the valleys). The influence of the Abbott–Firestone curve on the systematic offset due to surface roughness will be further analyzed in future works.

It is also relevant to notice that the experimental results presented in this work show that the voxel size does not influence the systematic error of surfaces analyzed in this paper. The three samples, in fact, were scanned at different

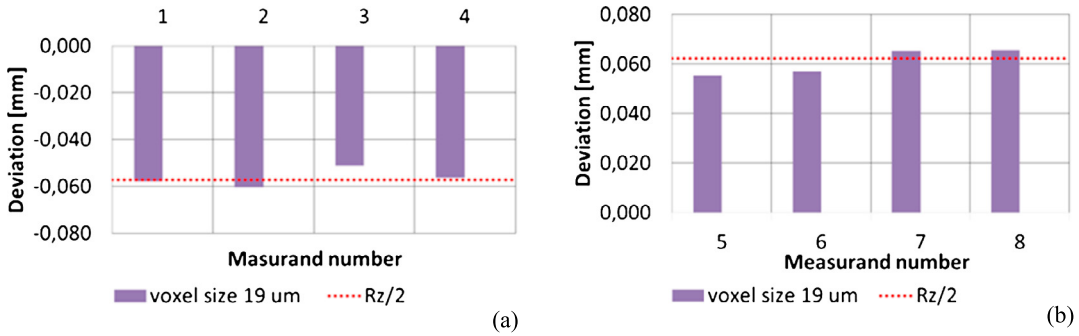

Fig. 5. (a) Deviations between CT and CMM measurements for external diameters of sample 2. Vertical columns represent the deviations for each measurand, while the horizontal axis represents the measurand number. The dashed line shows the value corresponding to *Rz*/2 of the external surface. (b) Deviations between CT and CMM measurements for internal diameters of sample 2. Vertical columns represent the deviations for each measurand, while the horizontal axis represents the measurand number. The dashed line shows the value corresponding to *Rz*/2 of the internal surface.

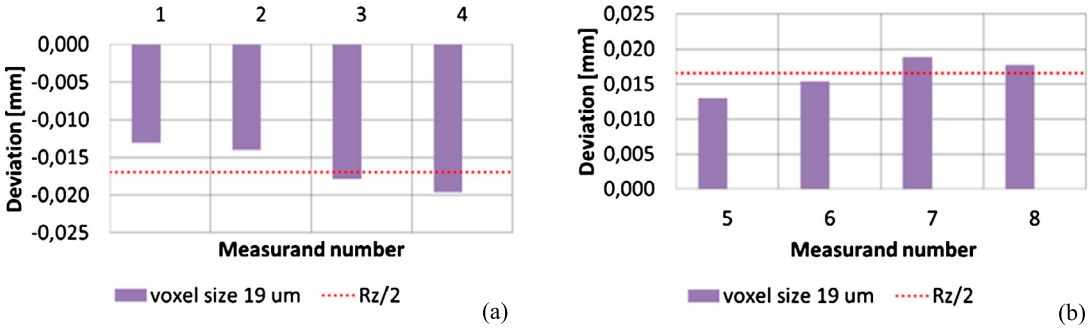

Fig. 6. (a) Deviations between CT and CMM measurements for external diameters of sample 3. Vertical columns represent the deviations for each measurand, while the horizontal axis represents the measurand number. The dashed line shows the value corresponding to *Rz*/2 of the external surface. (b) Deviations between CT and CMM measurements for internal diameters of sample 3. Vertical columns represent the deviations for each measurand, while the horizontal axis represents the measurand number. The dashed line shows the value corresponding to *Rz*/2 of the internal surface.

voxel sizes. For sample 1, which was scanned with a voxel size of 120 µm, that is of the same order of magnitude of the surface roughness parameter *Rz*, the systematic error is approximately *Rz*/2. For sample 2, instead, the voxel size is approximately 7 times smaller than the measured *Rz* value, but the systematic error remains approximately *Rz*/2. Finally, sample 3 was scanned with a voxel size slightly smaller than *Rz* (voxels size = 19 µm, *Rz* = 30 µm), and also in this case the systematic error remains approximately *Rz*/2. Further work is needed to determine the relation between the voxel size and the systematic error in other cases.

4.1. Correction of systematic errors due to roughness

The final part of this paper discusses the possibility to correct the systematic error due to roughness. Although the deviations between CT and CMM measurement results are due to the different acquisition principles of the two measuring techniques, and therefore cannot be attributed to CT only, CMM measurements are currently considered as reference when compared to CT measurements (as discussed above in Section 2). For this reason, in the following, CMM measurements are used as reference and, consequently, systematic errors due to roughness are intentionally attributed to CT. Therefore, in the following, the reference diameter is defined as the diameter measurable by CMM. This approach is useful especially in relation to industrial measurements, where CMMs are currently used to determine reference results to be compared with CT results.

According to the GUM ("Guide to the expression of Uncertainty in Measurement" [19]), systematic errors shall always be corrected for, and not considered in the uncertainty budget. However, for practical reasons, sometimes the bias is accounted for in the uncertainty budget. This was for example the approach suggested in the first version of ISO 15530-3 (ISO/TS 15530-3:2004 [20], which was then slightly changed in ISO/DIS 15530-3:2009 that is the document cited in [2]). In the current version (ISO 15530-3:2011 [4]), instead, the bias is not added to the uncertainty but is corrected for, in accordance to the GUM. The two different approaches for uncertainty evaluation (ISO 15530-3:2011 versus ISO/TS 15530-3:2004 or ISO/DIS 15530-3:2009) are compared in the following.

In the new approach described in ISO 15530-3:2011, the expanded measurement uncertainty *U* is determined by a series of repeated measurements, by Eq. (4.1):

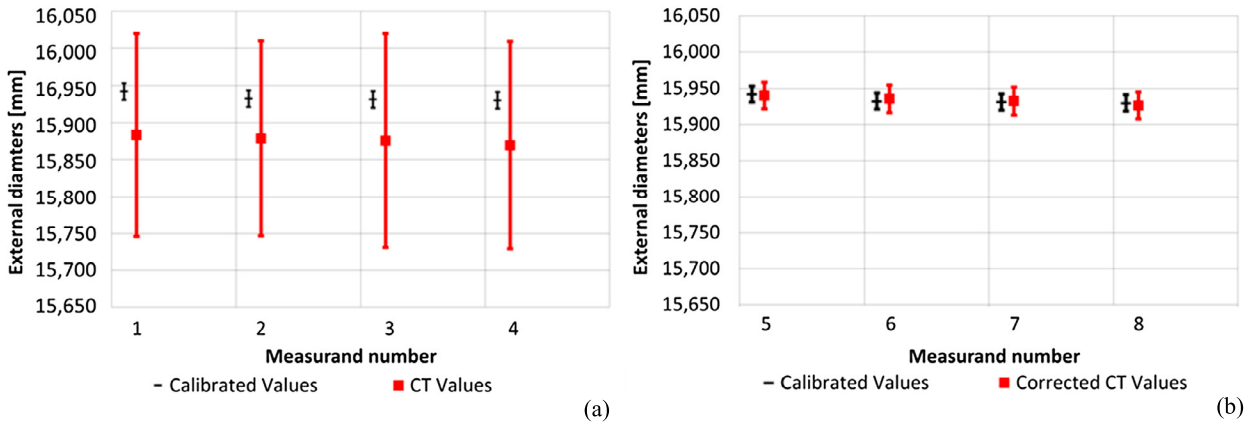

Fig. 7. Uncertainties of CT measurements for external diameters of sample 2, as determined from: (a) approach inspired by ISO/DIS 15530-3:2009; (b) approach inspired by ISO 15530-3:2011. For both diagrams, red error bars represent CT measurement uncertainty, while black error bars represent calibration uncertainty.

$$U = k \cdot \sqrt{u_{cal}^2 + u_p^2 + u_w^2 + u_b^2} \tag{4.1}$$

where k is the coverage factor, u_{cal} is the calibration uncertainty of the calibrated workpiece, u_p the uncertainty of measurement procedure, u_w the uncertainty associated with the influence of the workpiece (e.g. surface roughness, material and manufacturing variations, etc.), and u_b the uncertainty of the systematic error. According to this approach, the bias contribution b is not added to the expanded measurement uncertainty U.

Vice versa, in the old approach described in ISO/TS 15530-3:2004 and ISO/DIS 15530-3:2009, the bias is accounted for directly in the uncertainty budget. According to ISO/DIS 15530-3:2009 (which was the approach used also in [2]), the uncertainty is determined by Eq. (4.2):

$$U = k \cdot \sqrt{u_{cal}^2 + u_p^2 + u_w^2 + b^2} \tag{4.2}$$

where the bias contribution b is taken into account directly for determining the expanded measurement uncertainty U. This approach was used for example by Schmitt and Niggemann in [2]. There the uncertainty component due to surface roughness is assigned a rectangular distribution with limits $\pm Rz/2$, and then added to the uncertainty associated with the influence of the workpiece (u_w) which then contributes to the overall uncertainty (U) of CT measurements. The case study investigated in [2] is a workpiece with an average Rz of 6.82 µm, CT scanned with a voxel size of 145 µm. In that case, therefore, the roughness uncertainty component was not large, and the application of the ISO/TS 15530-3:2004 approach was possible without major consequences for the overall CT measurement uncertainty evaluation. However, when applying this approach also for parts characterized by high surface roughness, the u_w component could reach very high values and become the predominant component in the uncertainty budget, leading to a considerable overestimation of measurement uncertainty. This is the case for parts characterized by high surface roughness such as additive manufactured parts. Therefore, especially in this case, the authors recommend to always correcting the systematic errors due to roughness, in accordance to GUM and to ISO 15530-3:2011.

Fig. 7 shows results obtained from the 5 repeated measurements of sample 2. In Fig. 7-a CT values are represented with measurement uncertainty calculated according to the approach suggested in [2] (according to ISO/DIS 15530-3:2009). In this case, no correction of systematic errors is applied, the bias b is added to the CT uncertainty budget, and a rectangular distribution is assigned to the uncertainty component coming from surface roughness u_w as proposed in [2]. In this case, the bias b is the predominant contribution and produces a large overestimation of CT measurement uncertainty, which is on average 140 µm in Fig. 7-a. When ISO 15530-3:2011 is applied (Fig. 7-b), and systematic errors due to surface roughness are corrected, a significant decrease of CT measurement uncertainty is obtained, as visible by comparing Fig. 7-b to Fig. 7-a.

5. Conclusions

The effects of surface roughness on CT dimensional measurements have been evaluated by performing repeated CT scans on three different AM workpieces calibrated by means of a tactile CMM and characterized by Rz values ranging from 30 µm to 125 µm. Experimental results confirm that surface roughness causes a systematic error between CMM and CT measurements. External diameters are always smaller than the corresponding CMM reference values of approximately $Rz/2$, while internal diameters are always bigger than CMM values of approximately $Rz/2$. This systematic difference is caused by the different measuring principles on which tactile CMMs and CT rely on. The systematic difference caused by roughness is close to $Rz/2$ for all the surfaces analyzed in this work, which have similar bearing properties (i.e. similar Abbott–Firestone curves). This has been confirmed for several conditions: different CT systems (fan and cone beam), different workpiece

materials (metal and polymer), different AM processes (SLS and FDM), different roughness (*Rz* ranging from 30 µm to 125 µm), different voxel sizes (same order of *Rz*, approximately half of *Rz*, and seven times smaller than *Rz*). Further work is needed to determine the influence of the Abbott–Firestone curve on the systematic difference due to roughness, for surfaces with different bearing properties.

References

[1] Kruth JP, Bartscher M, Carmignato S, Schmitt R, De Chiffre L, Weckenmann A. Computed tomography for dimensional metrology. CIRP Ann – Manuf Technol 2011;60(2):821–42. http://dx.doi.org/10.1016/j.cirp.2011.05.006.

[2] Schmitt R, Niggemann C. Uncertainty in measurement for *X*-ray-computed tomography using calibrated work pieces. Meas Sci Technol 2010;21:054008.

[3] Fiedler D, Bartscher M, Hilpert U. Dimensionelle Messabweichungen eine industriellen 2D-Computertomographen: Einfluss der Werkstü ckrauheit. DGZfP; 2004.

[4] ISO 15530-3. Geometrical product specifications (GPS) – coordinate measuring machines (CMM): technique for determining the uncertainty of measurement – part 3: use of calibrated work pieces or measurement standards. Geneva: International Organization for Standardization; 2011.

[5] Bartscher M, Neukamm M, Hilpert U, Neuschaefer-Rube U, Härtig F, Kniel K, et al. Achieving traceability of industrial computed tomography. Key Eng Mater 2010;437:79–83.

[6] Carmignato S, Savio E. Traceable volume measurements using coordinate measuring systems. CIRP Ann – Manuf Technol 2011;60(1):519–22. http://dx.doi.org/10.1016/j.cirp.2011.03.061.

[7] Ontiveros S, et al. Dimensional measurement of micro-moulded parts by computed tomography. Meas Sci Technol 2012;23:125401. http://dx.doi.org/10.1088/0957-0233/23/12/125401.

[8] Yagüe-Fabra JA, et al. A 3D edge detection technique for surface extraction in computed tomography for dimensional metrology applications. CIRP Ann – Manuf Technol 2013;62(1):531–4. http://dx.doi.org/10.1016/j.cirp.2013.03.016.

[9] Müller P, Hiller J, Dai Y, Andreasen JL, Hansen HN, De Chiffre L. Estimation of measurement uncertainties in X-ray computed tomography metrology using the substitution method. CIRP J Manuf Sci Technol 2014;7:222–32.

[10] Bartscher M, Neukamm M, Koch M, Neuschaefer-Rube U, Staude A, Goebbels J, et al. Performance assessment of geometry measurements with micro-CT using a dismountable work-piece-near reference standard. In: Eur Conf on NDT (ECNDT). 2010.

[11] Boeckmans B, Tan Y, Welkenhuyzen F, Guo YS, Dewulf W, Kruth JP. Roughness offset differences between contact and non-contact measurements. In: 15th Euspen Int Conf and Exhib. 2015. p. 189–90.

[12] Carmignato S. Accuracy of industrial computed tomography measurements: experimental results from an international comparison. CIRP Ann – Manuf Technol 2012;61(1):491–4. http://dx.doi.org/10.1016/j.cirp.2012.03.021.

[13] ISO 10360-2. Geometrical product specifications (GPS) – acceptance and reverification tests for coordinate measuring machines (CMM) – part 2: CMMs used for measuring linear dimensions. Geneva: International Organization for Standardization; 2010.

[14] Trapet E, Savio E, De Chiffre L. New advances in traceability of CMMs for almost the entire range of industrial dimensional metrology needs. CIRP Ann – Manuf Technol 2004;53(1):433–8.

[15] Kerckhofs G, Pyka G, Moesen M, Schrooten J, Wevers M. High-resolution micro-CT as a tool for 3D surface roughness measurement of 3D additive manufactured porous structures. In: iCT Conf. 2012. p. 77–83.

[16] ISO 4288. Geometrical product specifications (GPS) – surface texture: profile method – rules and procedures for the assessment of surface texture. Geneva: International Organization for Standardization; 1996.

[17] Volume Graphics GmbH. http://www.volumegraphics.com/en/products/vgstudio-max/coordinate-measurement/ (accessed on 31/03/2016).

[18] ISO 13565-2. Geometrical product specifications (GPS) – surface texture: profile method; surfaces having stratified functional properties – part 2: height characterization using the linear material ratio curve. Geneva: International Organization for Standardization; 1996.

[19] JCGM 100. Evaluation of measurement data – guide to the expression of uncertainty in measurement. Joint Committee for Guides in Metrology; 2008.

[20] ISO/TS 15530-3. Geometrical product specifications (GPS) – coordinate measuring machines (CMM): technique for determining the uncertainty of measurement – part 3: use of calibrated workpieces or measurement standards. Geneva: International Organization for Standardization; 2004.